processes

MDPI

Article

Prediction of Winter Wheat Harvest Based on Back Propagation Neural Network Algorithm and Multiple Remote Sensing Indices

Hong Ji, Xun He, Wanzhang Wang * and Hongmei Zhang

College of Mechanical and Electrical Engineering, Henan Agricultural University, Zhengzhou 450002, China
* Correspondence: wangwz@henau.edu.cn

Abstract: Predicting the harvest time of wheat in large areas is important for guiding the scheduling of wheat combine harvesters and reducing losses during harvest. In this study, Zhumadian, Zhengzhou and Anyang, the main winter-wheat-producing areas in Henan province, were selected as the observation points, and the main producing areas were from south to north. Based on Landsat 8 satellite remote sensing images, the changes in NDVI (Normalized Difference Vegetation Index), EVI (Enhanced Vegetation Index), and NDWI (Normalized Difference Water Index) were analyzed at different growth stages of winter wheat in 2020. Multiple regression analysis and Back Propagation (BP) neural network machine learning methods were used to establish prediction models for the harvest time of winter wheat at different growth stages. The results showed that the prediction model based on a BP neural network had high accuracy. The RMSE, MAE and MAPE of the training set and the test set were 0.531 and 0.5947, 0.3001 and 0.3104, 0.0114% and 0.0119%, respectively. The prediction model of winter wheat harvest date based on BP neural network was verified in the main winter wheat producing areas of Henan province in 2020 and 2021. The average errors were 1.67 days and 2.13 days, which were less than 3 days, meeting the needs for winter wheat production and harvest. The grain water content of winter wheat at harvest time calculated by the prediction model reached the grain water standard of the wheat combine harvester. Therefore, the prediction of the winter wheat harvest time can be realized based on multiple remote sensing indicators.

Keywords: winter wheat; ripening; harvest period; remote sensing; vegetation index

check for updates

Citation: Ji, H.; He, X.; Wang, W.; Zhang, H. Prediction of Winter Wheat Harvest Based on Back Propagation Neural Network Algorithm and Multiple Remote Sensing Indices. *Processes* **2023**, *11*, 293. https://doi.org/10.3390/pr11010293

Academic Editors: Won Byong Yoon and Huai-Wen Yang

Received: 9 December 2022
Revised: 9 January 2023
Accepted: 10 January 2023
Published: 16 January 2023

Copyright: © 2023 by the authors. Licensee MDPI, Basel, Switzerland. This article is an open access article distributed under the terms and conditions of the Creative Commons Attribution (CC BY) license (https://creativecommons.org/licenses/by/4.0/).

1. Introduction

Winter wheat is one of the vital grain crops in China [1]. Predicting the date of harvesting winter wheat not only plays a guiding role in improving the efficiency of agricultural machinery [2] but also has significant implications in preventing and reducing losses in the late stage of wheat maturity. With the progress made in the country's rural land-transfer system, China has seen the transition of its traditional family-based model of crop planting, and scaled agricultural development has now become a reality [3]. During actual production and harvesting, combined with the forecast of the harvest period of winter wheat, the sequence of harvesting winter wheat can be effectively planned over a large area, and the harvesting machinery can be scheduled in advance, which is also a major sign of precision agriculture [4]. From the perspective of agronomy and high-yield harvesting, the indicator of harvesting for wheat harvesters is that, after the stage of dough ripeness, the grains become hard quickly, and at this moment, the harvest should be carried out immediately to achieve the ideally high yield. Otherwise, the harvest will be regarded as too late, in that not only the mass of 1000-grain is low, but also the moisture content of grains is lost at a severe level. In the meantime, the field is prone to grain losses, causing unnecessary production losses [5]. At present, farmers mainly rely on traditional experience to judge whether wheat is mature. Under such circumstances, they are prone to errors due

to subjective judgment, which is not suitable for the forecast of the ripening of wheat in a large area.

Through remote sensing, the ground information were quickly and accurately obtained in a relatively short period of time, so as to achieve ground observations in a large area and to obtain valuable data from remote sensing. Based on the forecast of the crop ripening period by satellite remote sensing, the valuable data were extracted from remote sensing that can indirectly reflect the images displayed during the ripening of crops [6]. The forecast of crop maturity based on varying images of satellite remote sensing were extensive researched. For instance, they have used remote sensing images from domestic satellite to reconstruct the time series of the NDVI (Normalized Difference Vegetation Index) so as to deduce the growth period of winter wheat and used the model of effective accumulated temperature to forecast the ripening of winter wheat [7]. Based on the data source of LAI (Leaf Area Index) of MODIS (Moderate-resolution Imaging Spectroradiometer), it was possible to forecast the ripening period of winter wheat by combining the heading date with the model of accumulated temperature-radiation through remote sensing inversion and to establish the models of accumulated temperature-radiation and LAI integral area to forecast the ripening period of maize [8]. The above studies involve the relatively single use of the vegetation index extracted by satellite remote sensing when drawing a conclusion on the forecast of the crop maturity period. Satellite remote sensing data were used to forecast the ripening of wheat based on changes in water and chlorophyll during the growth period. However, their scope of study is relatively small, so it is not suitable for forecasting the ripening period of winter wheat in a large area [9].

In addition, the models on crop growth were used to forecast crops' ripening period. The WOFOST (World Food Studies) model was used on crops to simulate the growth of winter wheat so as to forecast its ripening by optimizing input parameters, and they have realized the forecasting of winter wheat maturity in a large area [10]. Thanks to LAI (Leaf Area Index), the WOFOST model was applied and adapted for the winter wheat of North China to simulate the growth of winter wheat. The research has shown that the reinitialization of the emergence period has kept the time difference between the results of the simulated period of ripening and the actual period of emergence within the range of 2 d. After initialization, the model is able to forecast the ripening period of winter wheat more accurately [11]. However, the model of the growth of crops involves numerous parameters and massive calibration of parameters. Therefore, it is hard to obtain the information, such as soil types and crop varieties, necessary for forecasting crop ripening in a large area [12]. During winter wheat growth, meteorological factors can also be significantly influential. However, during the entire growth cycle of winter wheat, the amount of relevant meteorological data is massive, leading to correspondingly massive workloads when the data were analyzed. Studies have shown that changes caused by meteorological factors to the winter wheat during its growth period are shown by changes in relevant vegetation indices in an indirect manner [13–17]. The average changing trends of the three factors of MODIS–NDVI, temperature and precipitation tend to coincide, and they have all shown periodical features. The MODIS–NDVI has a positive correlation with climatic factors. The temperature could affect precipitation, and these two factors may affect MODIS–NDVI, leading to changes in plant growth and number [18–21]. The vegetation index (NDVI) of Huanxian county in the semi-arid area of Longdong in Gansu Province and the semi-humid area of Xifeng both showed a significant correlation with the standardized precipitation index SPI on varying time scales [22–24]. Based on the supervisory effects of different indices on the water content of winter wheat, the optimal index of monitoring water content in varying periods was selected. The study provides a theoretical basis for remote sensing in monitoring the water content of crops. Through our comprehensive analysis and comparison, it was found that the NDWI (Normalized Difference Water Index) is the most suitable index for monitoring the winter wheat after the flowering period and before the stage of milky ripeness, whereas NDVI is the most suitable index subsequent to the stage of milky ripeness [25–27]. This study attempts to

represent the influence of climatic factors on forecasting the period of wheat harvesting by selecting the vegetation index that can reflect the aforementioned climatic factors in an indirect manner.

Wheat harvesting has been referred to as the rush-harvest for a long time, and the word rush fully reflects its urgency. In the late stage of the dough ripeness of winter wheat, the grain attains the highest level of material accumulation, reaching physiological maturity before entering the dehydration stage [28–33]. For the wheat combine harvester to be applied, the water content of wheat to be harvested must range between 12% and 20%. Furthermore, when the water content of wheat grains ranges between 15% and 20%, it is regarded as the optimal harvesting period. The change in the water content of wheat is directly related to the determination of the time for harvesting wheat. The best time for this should be when the grain moisture decreases, and its hardness and mechanical resistance increase [34]. When it comes to the season with the most changing weather during the harvest, the wheat that meets the prescribed standards ought to be harvested as soon as possible to ensure the optimal returns of grains. This study extracted remote sensing indices (NDVI, EVI and NDWI) from Landsat 8 images to formulate a prediction model for the wheat harvest period. Compared with other prediction models, the Back Propagation (BP) neural network has unique performance and advantages and has become the most-used model in the field of artificial intelligence prediction [35]. In fact, 90% of neural network systems in practical applications use the BP algorithm. As the most commonly used algorithm model in the artificial neural network, the BP neural network has a relatively complete theoretical basis. It can imitate the reaction process of human brain neurons to external stimulation signals. Based on multi-layer perceptron, combined with the forward propagation of signals and the reverse regulation of errors, it can effectively establish an intelligent network prediction model for processing nonlinear information based on repeated learning [36].

In order to effectively guide the rational scheduling of cross-regional combine harvesters and improve the quality of wheat harvest in the field, this study focuses on the construction of a wheat harvest-time prediction model based on multiple remote sensing indices, which to a certain extent provides theoretical and technical support for regional wheat-harvesting-machinery scheduling.

2. Materials & Methods

2.1. Overview of the Research Area

The main area of planting winter wheat in Henan province is selected as the research area, whose geographical coverage is 31°23′ N~36°22′ N, 110°21′ E~116°39′ E. The total wheat planting area is 14.78335 × 10^6 hm^2 (according to data from the National Bureau of Statistics of China, 2018). Most regions of Henan province are located in the warm temperate zone, whereas the southern parts of the Province are in the subtropical zone, which features the continental monsoon climate typical during the transition from the northern subtropical zone into the warm temperate zone. As a result, the area has four distinct seasons, with moderate rainfall and sufficient sunlight. The average annual temperature in Henan province from south to north is 10.5~16.7 °C; the average annual precipitation falls in the range of 407.7~1295.8 mm, and the average annual sunlight exposure is 1285.7~2292.9 h (Central People's Government of the P.R.C., 2018). The local weather is suitable for the growth of winter wheat. In Henan province, the winter wheat is usually sown in October, turns green from February to March, heads in April, and is ready to be harvested from May to June. The growth period lasts for 215~235 d. There is a huge difference in light and heat conditions between the north and the south of Henan province. Therefore, it is suitable for researching and forecasting the period of harvesting winter wheat in a large area. To facilitate this prediction, three main producing areas of winter wheat as our major areas of research were selected, namely, Zhumadian, Zhengzhou and Anyang in the southern, central and northern parts of Henan province, respectively. In the southern area of Zhumadian, the experimental field in the Zhumadian Academy of Agricultural Sciences is

taken as the site of research, with geographic coordinates of north latitude 33°0′33″and east longitude 114°2′26″. In Zhengzhou, the central area of Henan province, the experimental field of the Henan Academy of Agricultural Sciences is taken as the observation point, with geographic coordinates of north latitude 35°0′33″ and east longitude 113°41′24″. In the northern area of Anyang City, the wheat-planting area to the east of the Anyang Academy of Agricultural Sciences of the Wadian Township of Anyang County is taken as the site of research, with geographical coordinates of north latitude 35°59′46″ and east longitude 114°32′1″, as shown in Figure 1.

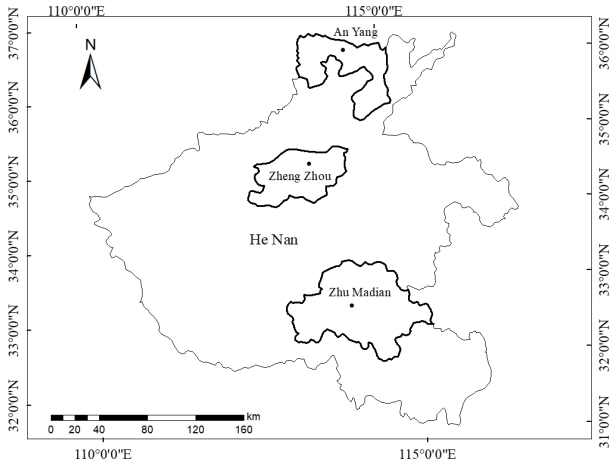

Figure 1. Distribution of research areas.

2.2. Research Data

2.2.1. Remote Sensing Data

The images extracted from the Landsat 8-OLI in 2020 are selected as the source of remote sensing data. The OLI land imager includes 9 bands, with a multi-spectral and panchromatic band spatial resolution of 30 m and 15 m, respectively. The satellite revisit period lasts for 16 d, and the width of imaging is 185 km × 185 km. ENVI 5.1, the software for processing remote sensing images, is used to preprocess the imaging data extracted from the Landsat 8-OLI. The preprocessing methods include radiometric calibration, atmospheric correction, image cropping, cloud removal processing, and converting the DN value of each band of the images into the reflectivity of ground objects. Since the seedlings of winter wheat are short during the stages of emergence and tillering, they are prone to disturbance by soil pixels when the vegetation index is extracted from satellite remote sensing images, compromising the accuracy of the forecast. Therefore, the stages of the elongation and ripening of winter wheat were mainly studied and analyzed. By selecting images of winter wheat during the stages of elongation and ripening in 2020, we have selected 23 scenes covering the main growth period of winter wheat with less cloud cover in the research area.

2.2.2. Remote Sensing Digital Images Extracted from Main Research Areas

In this study, remote sensing images from Zhumadian, Zhengzhou and Anyang of Henan province during three growth stages of winter wheat were extracted, namely, the elongation stage, the heading stage and the filling and maturation stage in 2020. The images include 12 scenes in Anyang, 6 scenes in Zhengzhou and 5 scenes in Zhumadian (Table 1).

Table 1. List of remote sensing images from Landsat 8 in main research areas in Henan province.

No.	Time	Research Area	No.	Time	Research Area
1	3 March 2020	Zhengzhou, Zhumadian	8	29 April 2020	Anyang, Zhumadian
2	12 March 2020	Anyang	9	6 May 2020	Anyang, Zhengzhou
3	19 March 2020	Anyang, Zhengzhou	10	15 May 2020	Anyang, Zhumadian
4	28 March 2020	Anyang, Zhumadian	11	22 May 2020	Anyang, Zhengzhou
5	4 April 2020	Anyang, Zhengzhou	12	31 May 2020	Anyang
6	13 April 2020	Anyang, Zhumadian	13	6 June 2020	Anyang
7	20 April 2020	Anyang, Zhengzhou			

2.3. Growth Periods of Winter Wheat in Henan Province

The varieties of winter wheat differ from each other from south to north in the main producing areas of Henan province. The southernmost area of Henan province is dominated by weak-spring wheat varieties, whereas the central and northern producing areas of wheat are dominated by semi-winter varieties. During the experiment, we have found limited discrepancy in the NDVI values among different varieties of winter wheat in the same period. Therefore, this study will rule out the influence of wheat varieties on forecasting winter wheat maturity.

Due to the varying climatic conditions from south to north in Henan province, the time nodes at different growth periods of winter wheat also vary to some extent. The distribution of the growth periods of wheat in the main research areas is shown in Table 2.

Table 2. The growth schedule of winter in the main research areas (elongation–maturation).

Observation Points	March			April			May			June		
	Early	Middle	Late	Early	Middle	Late	Early	Middle	Late	Early	Middle	Late
Zhumadian	Elongation Stage			Heading Stage	Filling Stage	Maturation Stage						
Zhengzhou	Elongation Stage			Heading Stage		Filling Stage	Maturation Stage					
Anyang	Elongation Stage					Heading Stage	Filling Stage	Maturation Stage				

2.4. Research Methods

Based on the spectral characteristics of the vegetation, we have combined the visible light and near-infrared bands of the satellite to form various vegetation indices [37]. In terms of remote sensing, the vegetation index has always been a simple and direct reference index used to quantify the coverage of surface vegetation and the status of growth. With the progress made in remote sensing technologies and the continuous expansion of field exploration, the vegetation index has been widely used in the distribution of crops, monitoring of growth, estimation of yield, monitoring of farmland disasters and early warning, regional environmental assessment and extraction of various biological parameters [38]. During the growth of winter wheat, canopy water and chlorophyll will obviously witness regular changes according to the different stages of growth and the influence of corresponding climatic factors. In addition, numerous studies have shown that, based on the remote sensing of the satellite and subject to meteorological factors, it can monitor the changes of crop chlorophyll through the normalized vegetation index (*NDVI)* and were able to respond to the changes in the canopy water by the normalized water index (*NDWI*).

The bands required by the *OLI* sensor for Landsat 8 satellite remote sensing images are divided into four bands, including near-infrared, red, blue and short-wave infrared. *OLI* sensor bands are shown in Table 3.

Table 3. Landsat 8 OLI sensor information by band.

Band	Wavelength Range (μm)	Spatial Resolution (m)
NIR	0.845–0.885	30
Red	0.630–0.680	30
Blue	0.450–0.515	30
SWIR	1.560–1.660	30

2.4.1. Calculation Method of Remote Sensing Index

In 1973, subsequent to the non-linear normalized processing of *RVI* (Ratio Vegetation Index), Rouse et al. obtained the Normalized Difference Vegetation Index (*NDVI*), which is a vital parameter that can well reflect the growth of crops [39]. The calculation formula is as follows:

$$NDVI = \frac{\rho_{NIR} - \rho_{red}}{\rho_{NIR} + \rho_{red}} \quad (1)$$

where,

ρ_{NIR} refers to the near-infrared band reflectivity,
ρ_{red} refers to the red-light band reflectivity.

Based on the ratio of the near-infrared and red-light bands, *NDVI* is prone to saturation and features limited treatment of atmospheric interference. In areas of low vegetation coverage, *NDVI* is easily affected by the soil background and vegetation canopy and is supersaturated in areas of high vegetation coverage. Herein, saturation refers to the phenomenon that the vegetation index no longer increases with vegetation growth when the vegetation coverage reaches a certain value. *EVI* has integrated such indices as ARVI (Atmospherically Resistant Vegetation Index) and SAVI (Soil Adjusted Vegetation Index) to correct the atmosphere and its residual aerosols and to help reduce the impact of the soil background. In addition, the index helps avoid the phenomenon of vegetation saturation, is able to sensitively monitor the growth and decline of both sparse and dense vegetation and can make up for the defects of *NDVI* [40]. The calculation formula is as follows:

$$EVI = \frac{2.5(\rho_{NIR} - \rho_{red})}{L + \rho_{NIR} + C_1\rho_{red} - C_2\rho_{blue}} \quad (2)$$

where,

ρ_{blue} refers to the blue-band reflectivity,
L refers to the soil regulation parameter, set as 1,
C_1 refers to the atmospherically corrected parameter with red-light correction, set as 6.0,
C_2 refers to the atmospherically corrected parameter with blue-light correction, set as 7.5.

The vegetation moisture index *NDWI* is the normalized ratio index based on the mid-infrared and near-infrared bands. Compared with *NDVI*, *NDWI* can effectively extract the water content of the vegetation canopy, and when the vegetation canopy is under water stress, the *NDWI* index can respond accordingly in time [41]. In terms of the images of the Landsat 8 OLI, short-wave infrared bands are used to represent mid-infrared bands. The calculation formula is as follows:

$$NDWI = \frac{\rho_{NIR} - \rho_{SWIR}}{\rho_{NIR} + \rho_{SWIR}} \quad (3)$$

where,

ρ_{NIR} refers to the near-infrared band reflectivity,
ρ_{SWIR} refers to the shortwave infrared band reflectivity.

2.4.2. Data Extraction from Ground Observation

Based on the research needs, ground observations and corresponding data measurements at the three selected observation points were carried out. According to the information on the planting of winter wheat at the three observation points (Table 4), the observation period was determined to be from 5 March 2020 to 10 June 2020. Specifically, the observation was carried out once every five days from the elongation stage to the heading and flowering stage of winter wheat. The observation was carried out once every two days from the filling stage to the early stage of ripening. In the meantime, the frequency of observation in the late stage of ripening was once a day.

Table 4. The growth period of winter wheat at observation points.

Observation Points	Sowing Date	Elongation Stage	Heading and Flowering Stage	Filling and Ripening Stage	Harvest Date	Growth Cycle (Day)
Zhumadian	23 October 2019	5 March 2020 to 2 April 2020	3 April 2020 to 15 April 2020	16 April 2020 to 23 May 2020	24 May 2020	215
Zheng zhou	16 October 2019	10 March 2020 to 9 April 2020	10 April 2020 to 24 April 2020	25 April 2020 to 28 May 2020	29 May 2020	227
Anyang	25 October 2019	15 March 2020 to 22 April 2020	23 April 2020 to 30 April 2020	1 May 2020 to 9 June 2020	10 June 2020	230

During ground observations, the *NDVI* data of the winter wheat canopy, using a Greenseeker handheld spectrometer (developed by Oklahoma State University in the United States and produced by Tremble), were measured. The Greenseeker handheld spectrometer can ensure that conditions are independent of time and atmospheric situation and is able to accurately measure and record the *NDVI* and ratio vegetation index (*RVI*). During the experiment of this research, the Greenseeker handheld spectrometer is used to measure the *NDVI* value of winter wheat during the stages of elongation, heading, and filling and ripening. The changes in the measured *NDVI* at the three observation points are shown in Figure 2.

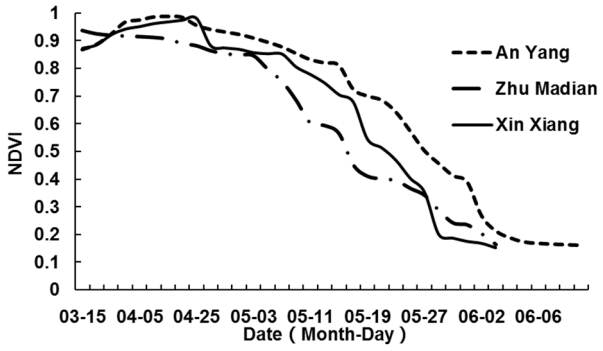

Figure 2. The chart of trend on the *NDVI* variation measured at the observation points.

2.4.3. Extraction of Data from Satellite Remote Sensing

Based on the remote sensing data provided by the satellite Landsat 8 and combined with the time recorded during ground observation, we obtained images from 5 March 2020 to 15 June 2020. The research used the Environment for Visualising Images (*ENVI*) 5.1 software to compute the *NDVI*, *EVI* and *NDWI* indices (1), (2) and (3). The vegetation indices *NDVI*, *EVI* and *NDWI* at the observation points are subject to variation during observation (Figure 3).

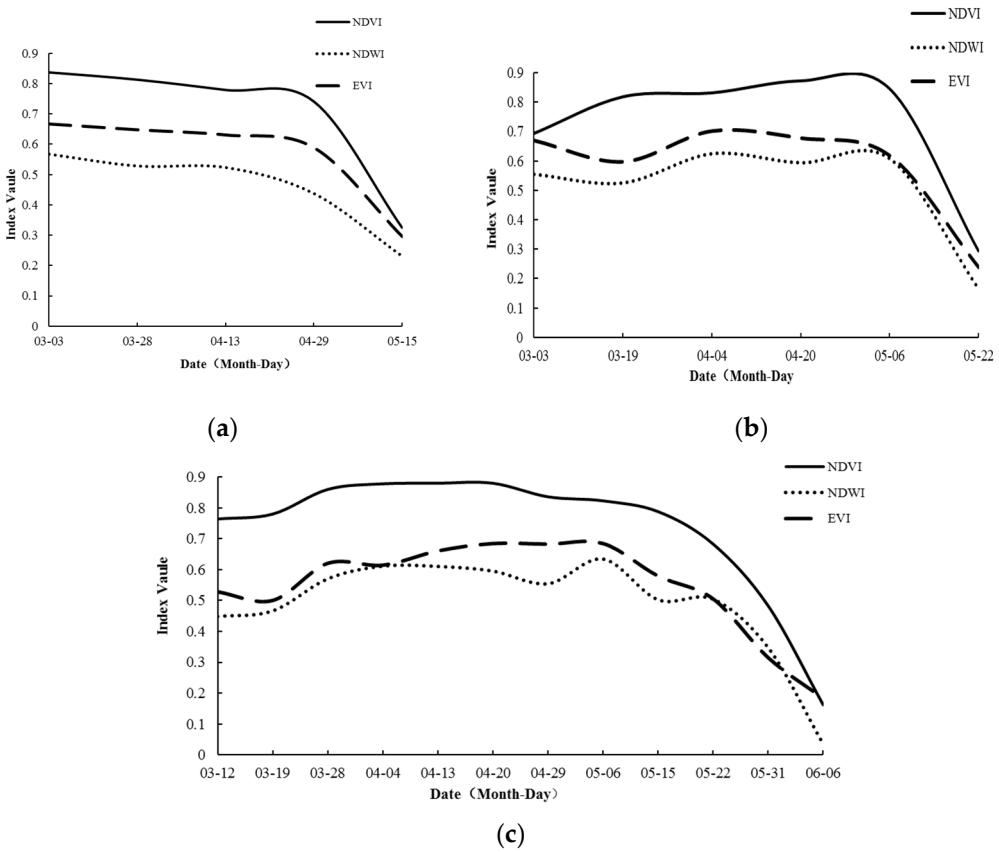

Figure 3. Chart of variation trend of *NDVI*, *NDWI* and *EVI* of Zhumadian (**a**), Zhengzhou (**b**) and Anyang (**c**) based on remote sensing data.

2.4.4. Multivariate Regression Analysis and Prediction Model for Winter Wheat Harvest

Judging from the previous analysis, the actual *NDVI* value measured at the ground observation points tend to be consistent with the changes in the *NDVI* value measured by satellite remote sensing. Remote sensing data from the geographic locations of the three observation points on the ground were the data source for predicting the winter wheat harvest period. Data extraction was from 3 March 2020 to 6 June 2020, considering the 23 scenes of *OLI* Level-1 and Level-2 of the Landsat 8 satellite. The regression analysis considered data pairs from remote sensing indices (independent variables) and ground observation (dependent variables). In addition, we adopted the multiple regression method to establish the model of forecasting the period of harvesting winter wheat during the elongation, heading and ripening stages. By analyzing the accuracy of the model in forecasting the harvest period at different growth periods of winter wheat, we can determine the model of forecasting the period of harvesting winter wheat.

2.4.5. Winter Wheat Harvest Time Machine BP Neural Network Machine Learning Prediction Model Construction Method

The pre-model of the wheat harvest used the BP neural network. BP network is one of the most widely used neural networks. It is a typical hierarchical network. It is composed of an input layer, hidden layer and output layer, and each neural unit is connected with each other. The BP network model realizes the assumption of multi-layer network learning. When the network gets a given external input, it passes from the input layer unit to the hidden layer unit. After processing by the hidden layer unit, it is sent to the output layer unit, and an output quantity is generated after processing by the output layer unit. If there is an error between the output response and the expected output sample, and the requirements are not met, then the error is transmitted backward, that is, the error value is

transmitted backward along the connection path layer by layer, and the connection weights of each layer are revised until the requirements are met [42].

Determining the number of implicit layers of the BP neural network and the number of neurons in each implicit layer is important for the overall neural network structure. In order to prevent the underfitting and overfitting of the model, the number of neurons in the implicit layers is determined according to the following empirical equation [43]:

$$N_h = \frac{N_s}{\alpha \times (N_i + N_o)} \quad (4)$$

where,

N_h is the number of neurons in the implicit layer.
N_i is the number of neurons in the input layer.
N_o is the number of neurons in the output layer.
N_s is the number of samples in the training layer.
α is a constant between 2 and 10.

The basic flow structure of BP neural network processing for winter wheat harvest prediction is shown in Figure 4.

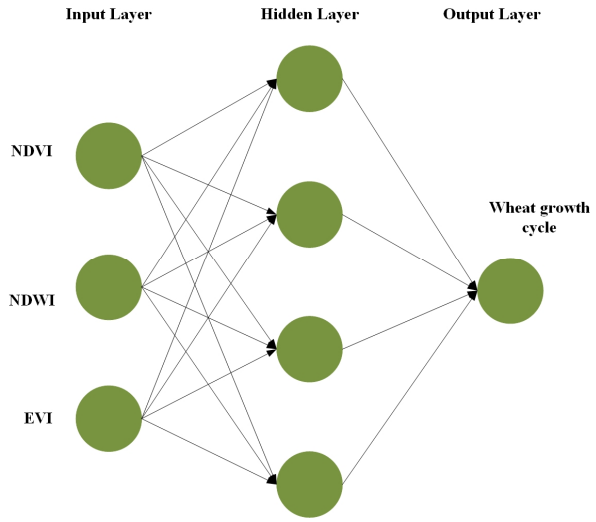

Figure 4. BP neural network structure and topology of the computational propagation process.

The output layer of the established neural network is the growth cycle of winter wheat; the input layers are three indices (*NDVI*, *NDWI* and *EVI*); the number of neurons in the input layer of the network is 3, and the number of neurons in the output layer is 1. This paper used a three-layer BP network to complete the mapping from three-dimensional input to one-dimensional output. The number of hidden-layer neurons is the key to the performance of the neural network system. Generally speaking, the more hidden-layer neurons, the higher the approximation ability of the network, but the increase in the number of neurons will lead to the decline in the network generalization ability.

2.4.6. Definition of the Optimal Period of Harvesting Winter Wheat

The main factor for judging the optimal date of winter wheat harvesting is the water content in wheat grains. When the water content of grains drops to 15%, the winter wheat should be harvested as soon as possible; otherwise, the winter wheat will be subject to yield losses and quality degradation. In addition, when the wheat combine harvester is working, the rate of water content in wheat grains is required to range between 12% and 20%. Taking into account the above two reasons, the optimal period of harvesting winter wheat is when the level of water content in grains ranges between 15% and 20%.

3. Result

3.1. Establishment of Multiple Linear Regression Prediction Model for Winter Wheat Harvest at Different Growth Stages

The forecast model for the winter wheat harvest period considered the sowing date as the first day of calculation, with the dates of the different phases of the winter wheat growing period converted into growing days to facilitate statistical analysis. Based on the remote sensing data of the satellite Landsat 8 *OLI* Level-1 and Level-2, the software of Design Expert 8.0.6 was used, took the winter wheat-related vegetation indices *NDVI*, *NDWI* and *EVI* at the observation points as independent variables and took the days of the winter wheat growth period as the dependent variables. In addition, we adopted the method of multivariate linear regression to establish the model of forecasting the period of harvesting winter wheat in the stages of elongation, heading and flowering, filling and ripening (Table 5).

Table 5. Model of forecasting varying growth stages of winter wheat.

Observation Points	Winter Wheat Growth Period	Forecasting Model	R^2	RMSE
Zhumadian	Elongation stage	$y = 824.23NDVI + 179.77NDWI - 423.4EVI - 377.14$	0.993	1.07
	Heading and flowering stage	$y = -45.12NDVI + 114.28NDWI - 260.13EVI + 314.98$	0.87	0.98
	Filling and ripening stage	$y = -59.09NDVI - 33.75NDWI + 51.13EVI + 218.39$	0.998	0.78
Zhengzhou	Elongation stage	$y = 91.57NDVI + 384.76NDWI - 213.6EVI + 6.69$	0.998	1.21
	Heading and flowering stage	$y = -6.3\text{NDVI} + 257.71\text{NDWI} + 40.94\text{EVI} + 12.32$	0.956	0.66
	Filling and ripening stage	$y = -83.76NDVI + 71.81NDWI - 3.13EVI + 233.15$	0.999	0.67
Anyang	Elongation stage	$y = 252.17.04NDVI + 208.14NDWI + 2.2.25EVI + 133.61$	0.938	5.84
	Heading and flowering stage	$y = -241.36NDVI - 310.1NDWI - 184.59EVI + 281.16$	0.88	1.9
	Filling and ripening stage	$y = 33.03NDVI - 7.23NDWI - 90.92EVI + 235.07$	0.989	1.29

By comparing the multiple regression models at different stages of the growth period of winter wheat at the three observation points, it was found that the determination coefficients of winter wheat grown in Zhumadian, Zhengzhou and Anyang at the ripening stage are higher than winter wheat during the stages of elongation, heading and flowering. Specifically, the coefficient of determination and the root mean square error (RMSE) of the aforementioned three stages are: $R^2 = 0.998$, RMSE = 0.78; $R^2 = 0.999$, RMSE = 0.67; $R^2 = 0.989$, RMSE = 1.29, respectively. The data prove that the *NDVI*, *NDWI* and *EVI* indices in the ripening stage of winter wheat have a relatively good fitting effect, and these indices are highly accurate in forecasting the period of harvesting winter wheat.

3.2. Establishment of Multiple Linear Regression Prediction Model for Winter Wheat Harvest in Henan Province

Based on the comparative analysis of the forecast models for varying stages of the growth period of winter wheat at the observation points, the satellite remote sensing data of winter wheat at the grain-filing and ripening stage from the three observation points in Zhumadian, Zhengzhou and Anyang from south to north in Henan province was integrated. In addition, the model of forecasting the period of harvesting winter wheat in a

large area of Henan province by using the satellite remote sensing data of winter wheat in the grain-filing and maturation satge, filling stage and maturity stage. Our analysis shows that the accuracy of the forecasting model established in the maturity stage of winter wheat in Henan province is relatively high, with a coefficient of determination R^2 = 0.97 and a root mean square error (RMSE) of 2.23 (Table 6). The results demonstrated that the range that the range of the independent variable is the maturity period of winter wheat, and the model of forecasting the period of harvesting winter wheat harvest based on the NDVI, NDWI and EVI vegetation indices in Henan province is as follows:

$$y = -16.85NDVI + 215.23NDWI - 536.14EVI + 320.2 \quad (5)$$

Table 6. Forecasting model of the filling and ripening stage of winter wheat in Henan province.

Winter Wheat Growth Period	Forecasting Model	R^2	RMSE
Grain-filling and maturation stage	y = 40.89$NDVI$ + 19$NDWI$ − 129.40EVI + 235.1	0.81	6.6
Filling stage	y = −193.67$NDVI$ − 8.44$NDWI$ − 119.08EVI + 121.35	0.958	3.39
Maturity stage	**y = −16.85$NDVI$ + 215.23$NDWI$ − 536.14EVI + 320.2**	**0.97**	**2.23**

3.3. Establishment of BP Neural Network Machine Learning Prediction Model for Winter Wheat Harvest in Henan Province

The BP neural network machine learning method was used to train the prediction model; the wheat harvest period of observation points in Henan province, namely the wheat growth cycle, was selected as the training samples, and a total of 435 samples were selected; the ratio of the training set to the test set was 7:3. BP neural network sample data statistics are shown in Table 7.

Table 7. Wheat growth cycle value characterization statistics.

Type of Samples	Number of Samples	Min	Max	Mean	Standard Devitation
Training	305	183	204	198	9.85
Validation	130	197	219	210	6.59
Overall	435	183	219	200	10.34

When the number of implied neurons reached five, the BP neural network accuracy was the highest among all implied neurons, with the RMSE, MSE, MAE and MAPE of the training set and test set being 0.531 and 0.5947, 0.3001 and 0.3104, 0.0114% and 0.0119%, respectively, as shown in Table 8. Thus, the BP neural network model can be applied to predict winter wheat harvest on a large scale; although the number of samples is low, the algorithm still showed a good performance. In summary, the accuracy of the BP neural network model with five neurons in the hidden layer was better than all other models, and it was the most suitable model for predicting the winter wheat harvest.

Table 8. BP neural network machine learning training results.

Implied Number of Neurons	Training Set			Test Set		
	RMSE	MAE	MAPE (%)	RMSE	MAE	MAPE (%)
3	0.8694	0.5668	0.0204	0.8290	0.5524	0.0192
4	0.5949	0.3508	0.0133	0.6790	0.4075	0.0150
5	**0.5310**	**0.3001**	**0.0114**	**0.5947**	**0.3104**	**0.0119**
6	0.6001	0.3131	0.0121	0.5446	0.3208	0.0121
7	0.6170	0.3336	0.0128	0.5961	0.3194	0.0119
8	0.5864	0.2981	0.0115	0.6595	0.3694	0.0139
9	0.4099	0.2392	0.0092	0.9711	0.4505	0.0171

3.4. Evaluation of BP Neural Network Machine Learning Prediction Model

Regression analysis of the prediction model of wheat grain moisture content was based on the BP neural network algorithm (Figure 5). The fitting degree R of the actual moisture content and the predicted moisture content of the training set, test set and all data sets are 0.99141, 0.99427 and 0.9918, respectively, and R is close to 1, which proves that the prediction accuracy of the wheat growth cycle based on the BP neural network algorithm is high.

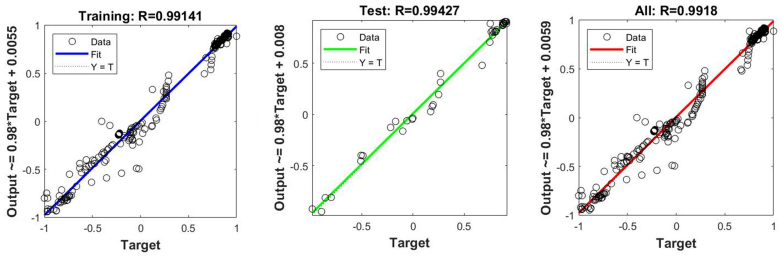

Figure 5. Regression prediction of wheat-growth-cycle prediction model.

4. Discussion

4.1. Interpretation of Result

The prediction models established by multiple linear regression and BP neural network machine learning were compared and analyzed, with vegetation index *NDVI*, *NDWI* and *EVI* as feature sets and wheat harvest time as the target variable. The R^2 of the prediction model based on multiple regression was 0.97, and RMSE was 2.23. R^2 = 0.99 and RMSE = 0.59 of the prediction model based on BP neural network machine learning, as shown in Table 9. Comprehensive analysis shows that the accuracy of the wheat-harvest-time prediction model based on the BP neural network method is significantly greater than that of the multiple linear regression model, indicating that the model was suitable for the prediction of winter wheat harvest.

Table 9. Comparison of prediction models for wheat moisture content at maturity stage.

Prediction Model	R^2	RMSE
Multiple linear regression	0.97	2.23
BP neural network machine learning	**0.99**	**0.59**

4.2. Validation of the Prediction Model

This study started by collecting relevant data on the period of harvesting winter wheat in Henan province in 2020 and 2021. To verify that the forecasting model is widely applicable, based on Landsat 8 OLI Level-1 and Level-2, the remote sensing images of nine regions (as shown in Figure 6) in the major producing areas of winter wheat during the harvesting period in 2020 and 2021 were obtained. The research areas include Nanyang,

Shangqiu, Luohe, Xuchang, Xinxiang and Puyang, which are located from south to north in Henan province. In addition, the vegetation indices *NDVI*, *NDWI* and *EVI* were extracted from the remote sensing images of nine regions and the verified data from the model for forecasting the period of harvesting winter wheat in Henan province. During data verification, we determined the growth cycle of winter wheat in the research areas by the method specified as follows. Firstly, the winter wheat sowing date of the observation site was provided by the regional Agricultural Science Institute. Secondly, the winter wheat harvest date at the observation site was obtained by using an IOT (internet of things) system of wheat combine harvester product measurement.

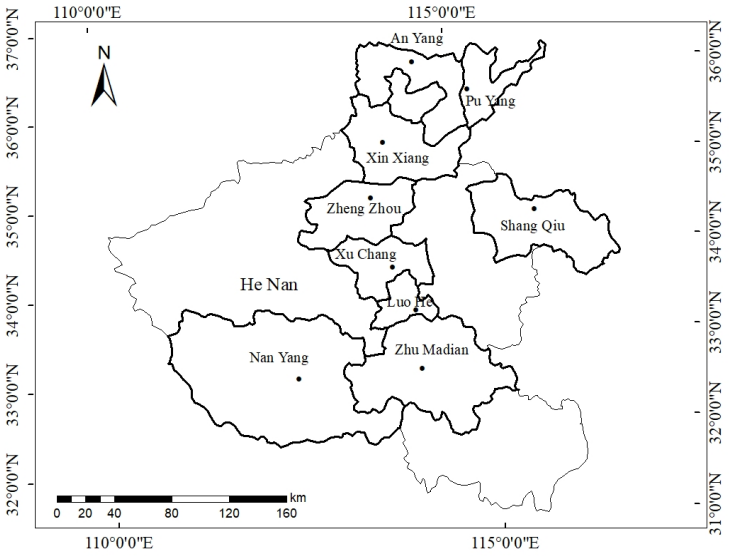

Figure 6. Producing areas of winter wheat that went through the verification in Henan province.

4.2.1. The Prediction Model Was Verified to Predict the Wheat Harvest Time in the Main Wheat-Producing Areas of Henan Province in 2020

First, except Zhumadian, Zhengzhou and Anyang, the remote sensing data of the satellite Landsat 8 from six major winter-wheat-producing areas in Henan province in 2020 were collected, namely, Nanyang, Shangqiu, Luohe, Xuchang, Xinxiang and Puyang. Furthermore, the data were imported into the forecasting model. Subsequently, it verified the data through the model of forecasting the period of harvesting winter wheat in Henan province. As shown in Table 10 and Figure 7, the average error is 1.67 d, and the coefficient of determination $R^2 = 0.932$, which meets the requirements of accuracy for the forecasting before harvesting winter wheat. Through our comparative analysis, it found that the error was rather large while forecasting the period of harvesting winter wheat in the producing areas in southern Henan province, as evidenced by the fact that $\Delta d = 3$. Due to the high temperature at the end of May and, in particular, the abnormally high temperature in southern Henan province, the local temperature increase was also rather huge compared with the central and northern regions, resulting in a larger error of the forecasting model. However, the error still falls within the proper range. Since the agricultural harvesting machinery in Henan province is operated from south to north in sequence, the error in forecasting the harvesting period in the southern will not affect the scheduling of the agricultural machinery to a large extent.

Table 10. Comparison of observed and forecasted values of the harvesting of winter wheat in Henan province in 2020.

Observation Points	Observed Value (Day)	Predicted Value (Day)	Error Value (Day)
Nanyang	224	227	3
Shangqiu	220	221	1
Luohe	222	220	−2
Xuchang	223	224	1
Xinxiang	234	236	2
Puyang	220	219	−1
Average error			1.67

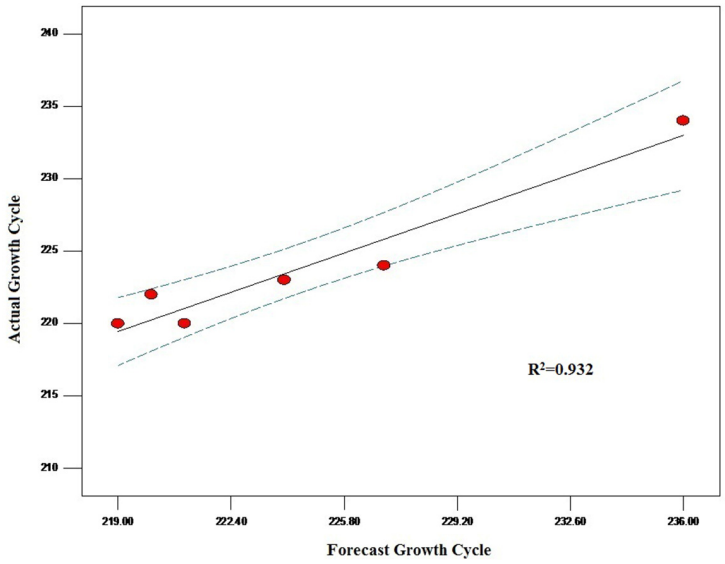

Figure 7. Scatter plot of forecasting the period of harvesting winter wheat in main producing areas of Henan province in 2020.

4.2.2. The Prediction Model Was Verified to Predict the Wheat Harvest Time in the Main Wheat-Producing Areas of Henan Province in 2021

The remote sensing data of the satellite Landsat 8 in the main winter-wheat-producing areas of winter wheat in Henan province in 2021 was imported into the forecasting model so as to verify the prediction accuracy. Since the remote sensing images of winter wheat in the ripening stage in Nanyang were fully covered by clouds, none of the remote sensing data for our verification were obtained. The verified winter-wheat-producing areas mainly include Zhumadian, Shangqiu, Luohe, Xuchang, Zhengzhou, Xinxiang, Puyang and Anyang from south to north in Henan province.

As shown in Table 11 and Figure 8, the average error of the model of forecasting the period of harvesting winter wheat in Henan province in 2021 is 2.13 d, and the coefficient of determination R^2 = 0.628, reaching a significant level of correlation. In addition, the forecasted value is relatively consistent with the observed value. According to Table 11, it was verified that, through the model of forecasting the period of harvesting winter wheat in Henan province, the corresponding grain water content of $NDVI_Y$ in the harvesting periods of winter wheat in 2021 both range between 15% and 20%, which is consistent with the requirements of forecasting the optimal period of harvesting winter wheat.

Table 11. Comparison of observed and forecasted values of harvesting winter wheat in Henan province in 2021.

Observation Points	Observed Value (Day)	Predicted Value (Day)	Error Value (Day)
Zhumadian	223	225	2
Shangqiu	226	223	−3
Luohe	230	229	−1
Xuchang	226	228	2
Zhengzhou	233	231	−2
Xinxiang	230	227	3
Puyang	230	233	3
Anyang	230	231	1
Average Error			2.13

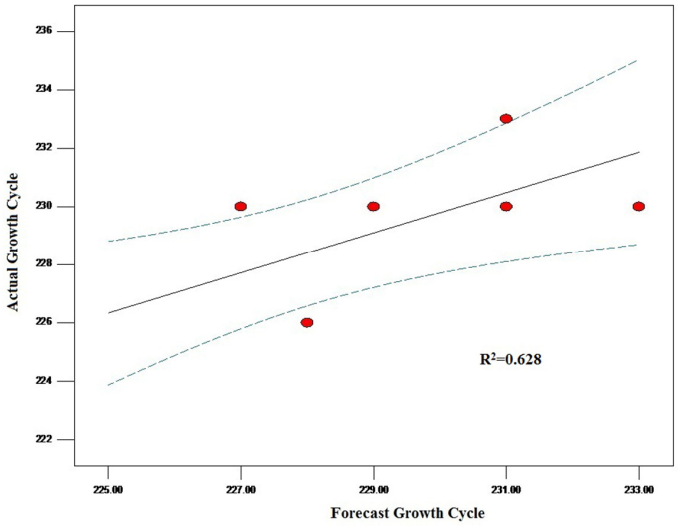

Figure 8. Scatter plot of forecasting the period of harvesting winter wheat in main producing areas of Henan province in 2021.

5. Conclusions

Based on Landsat 8 satellite remote sensing data, multiple linear regression and BP neural network prediction models were constructed with *NDVI*, *NDWI* and *EVI* as the characteristic quantities and the winter wheat growth cycle as the target variable. Through comparative analysis, the prediction model based on BP neural network has high accuracy, and the RMSE, MAE and MAPE of the training set and test set are 0.531 and 0.5947, 0.3001 and 0.3104, 0.0114% and 0.0119%, respectively. The winter wheat harvest-time prediction model based on the BP neural network was verified for the winter wheat harvest time in 2020 and 2021 in the main winter-wheat-producing areas of Henan province, and the average errors were 1.67 d and 2.13 d, and the error days were less than 3 d, which met the requirements of winter wheat production and harvest and can be widely used in the practical application of winter wheat harvest-time prediction. The results can effectively ensure the harvest of winter wheat in Henan province at the appropriate harvest period and rationally dispatch the combine harvester to maximize the utilization of resources. Based on Landsat 8 satellite remote sensing data, a multiple linear regression and BP neural network prediction model was constructed with *NDVI*, *NDWI* and *EVI* as the characteristic quantities and winter wheat growth cycle as the target variable. Through comparative analysis, the prediction model based on BP neural network has high accuracy, and the RMSE, MAE and MAPE of the training set and test set are 0.531 and 0.5947, 0.3001 and 0.3104, 0.0114% and 0.0119%, respectively. The winter wheat harvest-time prediction model based on the BP neural network was verified for the winter wheat harvest time in 2020 and 2021 in the main winter-wheat-producing areas of Henan province, and the average errors

were 1.67 d and 2.13 d, and the error days were less than 3 d, which met the demand of winter wheat production and harvest and can be widely used in the practical application of winter wheat harvest-time prediction. Through the results of this study, the harvest of winter wheat in Henan province at the appropriate harvest period can be effectively ensured, and the combine harvester can be rationally dispatched to maximize the utilization of resources.

Author Contributions: H.J.: conceptualization, data curation, writing—original draft and editing. X.H.: review and editing. W.W.: review and editing. H.Z.: review and editing. All authors have read and agreed to the published version of the manuscript.

Funding: This research was funded by Special Project for the Construction of Modern Agricultural Industrial Technology System (CARS-03) and Special Project of Modern Agricultural Industry Technology System in Henan (S2019-02-G07).

Institutional Review Board Statement: Not applicable.

Informed Consent Statement: Not applicable.

Data Availability Statement: The datasets used and/or analyzed during the current study are available from the corresponding author on reasonable request.

Conflicts of Interest: It is declared by the authors that this article is free of conflicts of interest.

References

1. Li, B.J.; Wang, T.H. Dual quantitative analysis of effects of meteorological factors on yield of winter wheat at different growth stages. *J. Triticle Crops* **2018**, *4*, 487–492.
2. Huang, J.X.; Wang, X. *Research on Remote Sensing Prediction Method of Regional Winter Wheat Maturity for Agricultural Machinery Navigation and Scheduling*; GNSS and LBS Association of China: Beijing, China, 2016; pp. 172–178.
3. Chen, L.Q. Research on the new mode of rural land transfer. *Agric. Mach. Agron.* **2020**, *51*, 74.
4. Chunjiang, Z.; Xuzhang, X.; Xiu, W.; Liping, C.; Yuchun, P.; Zhijun, M. Research progress and prospect of precision agriculture technology system. *Trans. CSAE* **2003**, *4*, 7–12.
5. Xue, C.L.; Yi, Q.X.; Zhang, C.S. Variation law of different harvesting time on thousand-kernel weight in wheat. *J. Shanxi Agric. Sci.* **2014**, *42*, 667–668+682.
6. Meng, J.H. Crop growth monitoring. *Remote Sens.* **2006**, *14*, 4565.
7. Huang, J.X.; Niu, W.H.; Ma, H.Y.; Huang, R.; Zhu, D.H. Prediction of maturity data for winter wheat based on time series of HJ-1 A/B CCD images. *Trans. Chin. Soc. Agric. Mach.* **2016**, *47*, 278–284.
8. Huang, J.X.; Wang, L.; Huang, R.; Huang, H.; Su, W.; Zhu, D.H. Forecastin of regional maize maturity using accumulated temperature-solar radiation model and leaf area index integral area model. *Trans. Chin. Soc. Agric. Mach.* **2019**, *50*, 133–143.
9. Meng, J.H.; Wu, B.F.; Du, X.; Dong, T.F.; Niu, L.M. Predicting mature date of winter wheat with HJ-1A/1B data. *Trans. CSAE* **2011**, *27*, 25–230.
10. Huang, J.X.; Gao, X.R.; Huang, H.; Ma, H.Y.; Su, W.; Zhu, D.H. Regional winter wheat maturity date prediction based on MODIS and WOFOST model data assimilation. *Trans. Chin. Soc. Agric. Mach.* **2019**, *50*, 186–193.
11. Ma, Y.P.; Wang, S.L.; Zhang, L.; Hou, Y.Y. A preliminary study on the re-initialization/re-parameterization of a crop model based on remote sensing data. *Chin. J. Plant Ecol.* **2005**, *6*, 52–60.
12. Meng, J.H.; Wu, B.F. The feasibility analysis on satellite data based crop mature data prediction. *Remote Sens. Technol. Appl.* **2013**, *28*, 165–173.
13. Chen, Q.L.; Xie, M.J.; Li, J.P.; Li, Z.; Zhang, M.L.; Wang, S.T. Change of vegetation NDVI and its response to meteorological elements in Hebei Province. *For. Ecol. Sci.* **2020**, *35*, 17–24.
14. He, H.; Zhang, B.; Hou, Q.; Li, S.; Ma, B.; Ma, S.Q. Variation of NDVI and its response to extreme temperature in the growing season of North China from 1982 to 2015. *Arid. Zong Res.* **2020**, *37*, 244–253.
15. Li, Y.; Du, L.; Yang, J.; Sun, H. Prediction of Wheat Mature Time Based on Temperature Index during Specific Growth Stage. *Chin. J. Agrometeorol.* **2012**, *33*, 104–108.
16. Lian, Z.; Zhao, S.; Kuang, S. Application of Phenological Observation Data in Forecast of Suitable Harvest Period of Wheat. *Chin. J. Agrometeorol.* **2006**, *3*, 226–228.
17. Hou, X.; Sui, X.; Yao, H.; Liang, S.; Wang, M. Response of Winter Wheat Phenology to Climate Change in Northern China. *J. Triticeae Crops* **2019**, *39*, 202–209.
18. Li, Z.; Yang, D.H.; Yuan, W.T. Coupling Relationship Between MODIS-NDVI and Climatic Factor. *Henan Sci.* **2014**, *32*, 737–740.
19. Wang, S.; Zhang, K.; Chao, L.; Li, D.; Tian, X.; Bao, H.; Xia, Y. Exploring the utility of radar and satellite-sensed precipitation and their dynamic bias correction for integrated prediction of flood and landslide hazards. *J. Hydrol.* **2021**, *603*, 126964. [CrossRef]

20. Liang, Y.; Jin, W.Y.; Guo, N.; Liu, S.X.; Han, T. Study on correlation between NDVI and precipitation in Longdong. *Agric. Res. Arid. Areas* **2009**, *27*, 247–251.
21. Liu, Y.; Zhang, K.; Li, Z.; Liu, Z.; Wang, J.; Huang, P. A hybrid runoff generation modelling framework based on spatial combination of three runoff generation schemes for semi-humid and semi-arid watersheds. *J. Hydrol.* **2020**, *590*, 125440. [CrossRef]
22. Chao, L.; Zhang, K.; Wang, J.; Feng, J.; Zhang, M. A Comprehensive Evaluation of Five Evapotranspiration Datasets Based on Ground and GRACE Satellite Observations: Implications for Improvement of Evapotranspiration Retrieval Algorithm. *Remote Sens.* **2021**, *13*, 2414. [CrossRef]
23. Quan, Q.; Gao, S.; Shang, Y.; Wang, B. Assessment of the sustainability of Gymnocypris eckloni habitat under river damming in the source region of the Yellow River. *Sci. Total Environ.* **2021**, *778*, 146312. [CrossRef] [PubMed]
24. Zhang, K.; Ali, A.; Antonarakis, A.; Moghaddam, M.; Saatchi, S.; Tabatabaeenejad, A.; Moorcroft, P. The Sensitivity of North American Terrestrial Carbon Fluxes to Spatial and Temporal Variation in Soil Moisture: An Analysis Using Radar-Derived Estimates of Root-Zone Soil Moisture. *J. Geophys. Res. Biogeosci.* **2019**, *124*, 3208–3231. [CrossRef]
25. Zhao, T.; Shi, J.; Lv, L.; Xu, H.; Chen, D.; Cui, Q.; Zhang, Z. Soil moisture experiment in the Luan Riversupporting new satellite mission opportunities. *Remote Sens. Environ.* **2020**, *240*, 111680. [CrossRef]
26. Zhu, D.M.; Wang, H.; Liu, D.T.; Gao, D.R.; Liu, G.F.; Wang, J.C.; Gao, Z.F.; Lu, C.B. Characteristics of grain filling and dehydration in wheat. *Sci. Agric. Sin.* **2019**, *52*, 4251–4261.
27. Wang, P.; Wu, J.J.; Nie, J.L.; Kong, F.M.; Ding, H.Y.; Zhao, L.H. A Comparatively Study of the Capabilities of Different Vegetation Water Indices in Monitoring Water Status of Wheat. *Remote Sens. Land Resour.* **2010**, *3*, 97–100.
28. Zhao, T.; Shi, J.; Entekhabi, D.; Jackson, T.J.; Hu, L.; Peng, Z.; Kang, C.S. Retrievals of soil moisture and vegetation optical depth using a multi-channel collaborative algorithm. *Remote Sens. Environ.* **2021**, *257*, 112321. [CrossRef]
29. Tian, H.; Qin, Y.; Niu, Z.; Wang, L.; Ge, S. Summer Maize Mapping by Compositing Time Series Sentinel-1A Imagery Based on Crop Growth Cycles. *J. Indian Soc. Remote Sens.* **2021**, *49*, 2863–2874. [CrossRef]
30. Tian, H.; Wang, Y.; Chen, T.; Zhang, L.; Qin, Y. Early-Season Mapping of Winter Crops Using Sentinel-2Optical Imagery. *Remote Sens.* **2021**, *13*, 3822. [CrossRef]
31. Ji, H.; Wang, W.Z.; Chong, D.F.; Zhang, B.Y. CARS algorith m-based detection of wheat moisture content before harvest. *Symmetry* **2020**, *12*, 115. [CrossRef]
32. Guo, N. Vegetation index and its advances. *J. Arid. Meteorol.* **2003**, *4*, 71–75.
33. Shen, X.J.; Han, D.J.; Hou, B.C.; Ma, R. Discussion on classification and application of vegetation indices. *Comput. Era* **2016**, *12*, 17–20.
34. Schell, J.A.; Rouse, J.W.; Haas, R.H. Monitoring Vegetation Systems in the Great Plains with ERTS. In Proceedings of the Third Earth Resources Technology Satellite-1 Symposium, Washington, DC, USA, 10–14 December 1974; NASA: Washington, DC, USA, 1974; Volume 351, pp. 310–317.
35. Wang, H.H. *Prediction Model of Poplar Drying Rate and Shrinkage Rate Based on Support Vector Machine and BP Neural Network*; Northeast Forestry University: Harbin, China, 2022.
36. Xie, H. *Vehicle Speed Prediction Based on BP Neural Network and Its Optimization Algorithm*; Chongqing University: Chongqing, China, 2014.
37. Bai, Y.Y.; Gao, J.L.; Zhang, B.L. Monitoring of crops growth based on NDVI and EVI. *Trans. Chin. Soc. Agric. Mach.* **2019**, *50*, 153–161.
38. Gao, B.C. NDWI-A normalized difference water index for remote sensing of vegetation liquid water fromspace. *Remote Sens. Environ.* **1996**, *58*, 257–266. [CrossRef]
39. Qi, H.X.; Wu, Z.Y.; Zhang, L.; Li, J.W.; Zhou, J.K.; Zou, J.; Zhu, B.Y. Monitoring of peanut leaves chlorophyll content based on drone-based multispectral image feature extraction. *Comput. Electron. Agric.* **2021**, *187*, 106292. [CrossRef]
40. Taghizade, S.; Navid, H.; Maghsodi, Y.; Vahed, M.M.; Fellegarii, R. Predicting Wheat Harvest Time Using Satellite Images and Regression Models. *AMA* **2019**, *50*, 28–33.
41. Kewen, X.; Changbiao, L.; Junyi, S. An optimization algorithm for the number of hidden layer nodes of feedforward neural networks. *Comput. Sci.* **2005**, *10*, 143–145.
42. Baofeng, Z.; Qiuyan, C. Water detection data processing based on BP neural network. *J. Liaoning Inst. Technol.* **2006**, *3*, 158–160.
43. Meng, Z.J.; Liu, H.Y.; An, X.F.; Yin, Y.X.; Jin, C.Q.; Zhang, A.Q. Prediction model of wheat straw moistuecontent based on SPA-SSA-BP. *Trans. Chin. Soc. Agric. Mach.* **2021**, *12*, 1542.

Disclaimer/Publisher's Note: The statements, opinions and data contained in all publications are solely those of the individual author(s) and contributor(s) and not of MDPI and/or the editor(s). MDPI and/or the editor(s) disclaim responsibility for any injury to people or property resulting from any ideas, methods, instructions or products referred to in the content.